Modeling of the multi-wavelenght emission of the blazar S50716+714 during a bright flare

Lulić, Lorena

UNIVERSITY OF RIJEKA

FACULTY OF PHYSICS

Lorena Lulić

Modeling of the Multi-wavelength emission of the blazar S5 0716+714 during a bright flare

Bachelor Thesis

Rijeka, 2024

UNIVERSITY OF RIJEKA

FACULTY OF PHYSICS

UNDERGRADUATE STUDY PROGRAM IN PHYSICS
COURSE INFORMATICS

Bachelor thesis

Modeling of the Multi-wavelength emission of the blazar S5 0716+714 during a bright flare

Supervisors:

izv. prof. dr. sc. Marina Manganaro

Candidate:

Lorena Lulić

Rijeka, 11.10.2024.

Contents

Abstract

Nowadays Multiwavelength (MWL) astrophysics (and recently also Multi-messenger) is making immense progress in the understanding of the emission mechanism of several celestial objects. Collecting data from different telescopes observing the same target simultaneously is of paramount importance in the study of galactic and extragalactic sources. The advances in technology are enabling observations of non-thermal radiation produced in multiple objects, such as Active Galactic Nuclei (AGNs), binary systems, supernova remnants, clusters of galaxies, Gamma-ray bursts and also our Galactic Center. Many objects emit photons through the entire electromagnetic spectrum and that is why MWL campaigns are often organized in order to collect as much as possible simultaneous data. In those efforts numerous researchers and observatories collaborate together. In this work, I use two broadband Spectral Energy Distributions (SEDs) of an AGN named S5 0716+714, which is a BL Lac type blazar, during a particular bright flaring activity in 2015 that emitted photons from radio to the very-high-energy (VHE) gamma-rays. In that occasion, a theoretical modelling was applied, which was not entirely successful. Since modelling a broadband dataset is of high importance in order to shed light on the processes behind the broadband emission, I worked with a program named JeT-Set, written in C and python language, which is devoted to modelling and interpretation of SEDs from AGNs and widely used in this field of research. I applied a simple pure leptonic model, the Synchrotron Self Compton (SCC) model to the dataset. My results show that the dataset can not be reproduced by such a model, which was expected. However, it allowed me to learn how to use the code and interpret complex datasets in Multiwavelength astrophysics, and to review the activity of the source in that particular state of activity.

Keywords: blazars, AGN, very-high-energy gamma rays, non-thermal, S5 0716+714, BL Lacertae objects

Introduction

For many years now, astrophysicists collaborate to observe celestial objects simultaneously with different telescopes, in order to collect data in a Multi-wavelength (MWL) context. In fact, even if the behaviour of a source in a particular energy range can bring plenty of interesting results, expanding the study to the entire electromagnetic spectrum makes possible not only to appreciate the particularity of a specific observation with one kind of telescope, but also to understand more deeply the emission mechanism of that source, tracking back to the physics processes that allow the broadband emission. Not all the sources can be observed to emit photons in the entire electromagnetic spectrum. For that reason, scientists are eager to understand why some of them, in some particular case can emit non-thermal radiation up to very-high-energy (VHE, E>100 GeV) gamma-rays, and what are the physical processes behind that. Some sources, for instance, Active Galactic Nuclei (AGNs), can emit photons up to TeV energies during states of enhanced activities. The study of correlations between different energy bands is exceptionally appealing because it can provide information on violent processes of difficult theoretical interpretation. Astrophysicists organize MWL campaigns to collect simultaneous data from specific sources with many different telescopes, which work in different energy ranges, from radio to the VHE gamma-rays. They produce MWL lightcurves, which are plots of the flux detected by each telescopes evolving over the observation time. From MWL lightcurves they identify the most interesting states of activity, study correlations between lightcurves. and produce broadband Spectral Energy Distributions (SEDs). SEDs are fingerprints of each source in a particular moment/period of time. They are the key for the theoretical interpretation of the emission mechanism of many galactic and extragalactic sources. This interpretation is reached with the use of theoretical models tested on the dataset with advanced computing programs, such as JeTSet[1], AGNpy[2], naima[3] and others. Theoretical models are grouped in two main categories: leptonic and hadronic models. In the leptonic ones, the particles responsible for the broadband emission are electrons, while in hadronic models, there are also hadrons, such as protons involved. This work is organized as follows:
In Sec. 1 I will describe AGNs and their categorization. In Sec. 2 I will

[1]https://jetset.readthedocs.io/en/1.3.0/
[2]https://agnpy.readthedocs.io/en/latest/
[3]https://naima.readthedocs.io/en/latest/

present blazars and their characteristics. In Sec. 3 I will focus in particular on the blazar S5 0716+714 which is the object of my work. In Sec.4 I shortly describe the MAGIC telescopes and in Sec. 5 the program which I used to model the broadband SED of S5 0716+714. In Sec. 6 I list my results on the modelling of the dataset with a simple theoretical model named Synchrotron Self Compton (SSC). Finally, conclusions and future prospects are drawn in Sec. 7.

1 Active Galactic Nuclei

AGNs are extremely dense regions located at the centres of galaxies that release vast amounts of energy covering the total electromagnetic spectrum - from radio waves to very high-energy gamma rays. Even though only about 10% reaches gamma-rays. This immense energy output is generated by the accretion of matter onto a supermassive black hole at the galaxy's core. Black holes in question are at least 10^6 times heavier than the solar mass (which is $M_\bullet = 2 \times 10^{30}$ kg). The amount of matter accreting on the black hole varies over time, and that is what determines the intensity of nuclei activity. The accretion process is a very energy efficient one. Unlike stars, which are mostly emitting radiation from thermal processes, for active galactic nuclei radiation is a blend from both thermal and non-thermal processes. Light emitted from AGNs can be brighter than light emitted from all of the stars in the galaxy combined by several orders of magnitude. A galaxy where the AGN is stationed is called an active galaxy.

1.1 Composition

AGNs consists of:

- Supermassive black hole: largest type of black hole, the engine that powers an AGN
- Accretion disc: formed by diffuse material in orbital motion around a black hole
- Broad Line Region (BLR): Fast-moving gas in the vicinity of the black hole, producing broad emission lines
- Narrow Line Region (NLR): Slower-moving gas farther out, producing narrow emission lines
- Relativistic Jets: Extremely high-speed jets of particles emitted along the poles of the black hole
- Torus: Ring made out of dust and gas surrounding the AGN, obscuring some of the emission
- Coronal Region: Hot, ionized region that emits X-rays above the accretion disk

1.2 Redshift

Redshift is a measure of how much the light emitted from the source has been stretched due to the expansion of the universe. Since AGNs are travelling opposite of Earth direction, main cause of redshifts is relativistic Doppler effect. We calculate it by given formula:

$$z = \frac{\lambda_{obsv} - \lambda_{emit}}{\lambda_{emit}}$$

AGNs are mostly found millions to billions of light years away from our planet Earth. The closest one, Centaurus A (NGC 5128) is located at approximately 12 million light-years from Earth and its redshift is $z = 0.00183$ [1]. Farthest known AGNs are quasars that are observed at redshifts of $z > 7$, which means that they are seen as they were when the universe was less than a billion years old. These AGNs are located more than 13 billion light-years from Earth. For example, the quasar J0313-1806, one of the most distant known AGNs, is located about 13.03 billion light-years away from Earth and has a redshift $z = 7.642$ [2]. Taking that into consideration, exploring AGNs actually allows astrophysicists to explore early universe and its formative processes.

1.3 Jets

Some accretion discs produce relativistic jets - beams of ionised matter. They travel with great velocities, which can be close to the speed of light, so we can often notice effects of the special theory of relativity, such as relativistic beaming [3]. Distances that these jets travel reach beyond hundred of thousands parsecs.

1.4 Classification

The categorization of AGNs is very complex, as can be noted from the AGN unification diagram in Fig. 1.

Considering AGN's spectra and relative jet to Earth position, we classify them into groups:

- Quasars (quasi-stellar objects)
  They are the most luminous objects known in the universe. Currently, there is $\sim$ 900,000 known quasars, with redshift $0.056 < z < 7.642$. Quasars are primarily found in the early universe. They emit mostly non-thermal radiation throughout the entire electromagnetic spectrum.

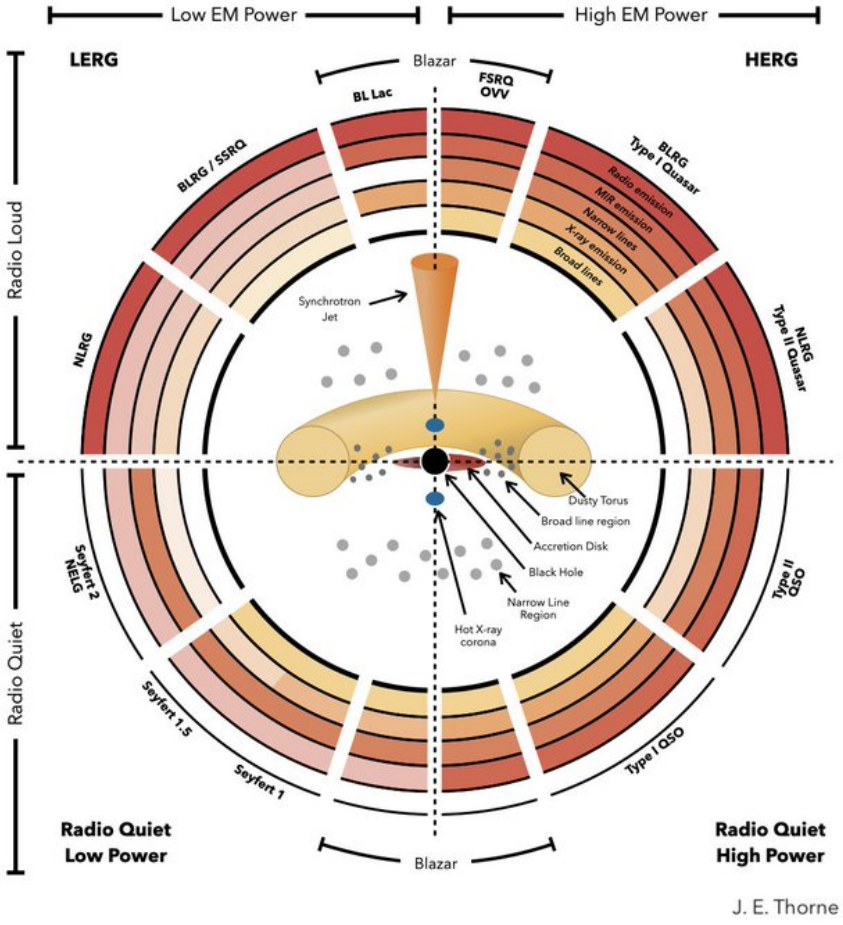

Figure 1: AGN unification diagram, from [4].

- Seyfert galaxies
  They resemble spiral galaxies in visible light and are occupying about 10% of the galaxies. They are not as luminous as quasars, and are a bit closer to the Earth. There are two classes of Seyfert galaxies (type 1 and 2), which we distinguish by differences in their emission spectra. In Seyfert 1 galaxies there are both broad and narrow emission lines, whereas in Seyfert 2 galaxies only narrow lines are found. Difference between their origin is not yet known.

- Radio galaxies
  They are characterised by emitting strong radio waves due to Synchrotron processes. Their host galaxies are most often elliptical.

- Blazars:
  They are the object of the next Section.

2 Blazars

Blazars are radio-loud AGNs that are characterized by having a relativistic jet pointed (almost) towards the observer. When first found, they have thought to be an irregular variable stars. According to unified AGN model, blazars are considered to be the same objects such as quasars, but viewed from a different angle. Galaxies hosting them are mostly elliptical [5]. They are highly variable in almost all energy bands, mostly due to changes in the jet. Their brightness can change rapidly over the course of just minutes.
SEDs of blazars commonly have two peaks [6]:

- lower-energy peak (radio to X-rays)
  which is a result from synchrotron radiation of the relativistic electrons spiralling around magnetic fields from the jet

- higher-energy peak (X-rays to VHE gamma rays)
  depends on the shape and position, but typically is a result of inverse Compton radiation from the same relativistic electrons transferring their energy to low-energy photons.

2.1 Flat Spectrum Radio Quasars

These types of blazars manifest strong emission lines in their optical spectra, indicating the presence of a more luminous accretion disk surrounding the central black hole. They commonly show higher overall energy output and have stronger gamma-ray emission than BL Lacs. For now, only 10 of them have been identified in the VHE gamma-ray band [7].

2.2 BL Lacs

Unlike FSRQs, BL Lacertae objects, abbreviated BL Lacs, have weak to no emission spectral lines. Powerful emission of BL Lac objects is explained as the result of a relativistic jet closely aligned with the line of vision, reported by [8]. Emission is non-thermal, dominated by synchrotron and inverse Compton scattering. We can further classify BL Lacs into low-energy peaked (LBL), intermediate (IBL) and high-energy peaked (HBL) depending on the position of their synchrotron peak. At this moment, about 400 objects are classified as BL Lacs [9].

3 S5 0716+714

3.1 Overview

The blazar S5 0716+714 is one of the brightest BL Lacs in the optical band. It is listed in the catalogue of TeV emitting sources [7][4]. Considering how the first SED peak varies between 10^{14} and 10^{15} Hz, blazar S5 0716+714 is classified as an intermediate peaked blazar (IBL) [10]. It is characterized by radical changes in most energy bands [11]. It is challenging to estimate its redshift due to a featureless optical continuum. However, the task has proved to be manageable using photometric detection of the host galaxy, and its redshift is approximately $z = 0.31 \pm 0.08$ [12].
Considering its high variability, it is often being observed by many different instruments. This specific blazar has the shortest known quasi-periodic oscillations, as concluded by [13], a $\sim$ 15-min quasi-periodic oscillations (QPOs) at optical frequencies. The source's variability has been extensively studied through optical monitoring [14], flux variability studies [15] and very long baseline interferometry (VLBI) observations [16].

3.2 Bright flare of 2015 in Multi-wavelength

In January 2015 the blazar S5 0716+714 was found in an enhanced state in many energy bands. A MWL campaign was organised and the results of those joint observations are reported in [17]. During that flaring activity, from the MWL lightcurves two Phases were modeled with a two-zone leptonic model. Phase A was from MJD 57040 (18/01/2015) to MJD 57050 (27/01/2015) and Phase B from MJD 57065 (12/02/2015) to MJD 57070 (17/02/2015). The reason to choose a two-zone model was connected to the fact that VLBI analysis was showing two shocks in the jet and those could be interacting and producing the VHE gamma-ray emission. The modelling was not very well reproducing the dataset so new models are being tested.

[4]https://heasarc.gsfc.nasa.gov/W3Browse/all/tevcat.html

4 The MAGIC telescopes

In this section, I will shortly write about technical implementation of MAGIC telescopes, since they are the the tool crucial for our observations. Information I used can be found on the MAGIC official web pages[5] [6]. MAGIC is a two telescopes system (MAGIC-I and MAGIC-II) found on the La Palma island in the Canary archipelago. The location on top of the volcano in the Atlantic ocean enables an almost completely undisturbed view of the night sky. The subtropical climate on the 28th latitude provides the optimal conditions for astronomical observations. The MAGIC telescopes are shown in Fig. 2. The two telescopes function in stereo mode since 2012. Cherenkov telescopes detect VHE gamma-rays from both galactic and extragalactic sources using the atmosphere as the medium. Compared to other telescopes of the same sort, The MAGIC telescopes stand out due to the improved and more sophisticated equipment, especially because of its mirrors and cameras. At the time of construction, in 2003., MAGIC telescope had largest mirrors with a active surface area of 236m^2 together with the best available photomultiplier tubes that provided a quantum efficiency around 30% which made it was the best light collector. In 2012, MAGIC-II was built, which doubled the mirror surface area. Subsequently, MAGIC became a much more sensitive telescope system to the electromagnetic showers of lower energy. With the simultaneous data analysis from the two telescopes, the sensitivity to the lower energy EM and Gamma-rays is enhanced.

4.1 Camera

The camera is mounted on a single aluminium tubular arc, secured against transverse movements by pre-stressed steel cables. Like all other components of the telescopes, its cameras were also intended to weigh as little as possible. That is accomplished by applying aluminium and thin steel supporting elements. Each telescope has its own hexagonal camera with 1039 photomultiplier tubes (PMTs) which are arranged in a circular shape with a diameter of approximately 1 m. With this, the field of view of each camera is 3.5 degrees. PMTs have a diameter of 25.4 mm. They are constituted from of a hemispherical photocathode and 6 dynodes, with a hexagonal Winston cone mounted on top to increase the amount of collected light and to avoid gaps between the circular pixels.

[5] https://magic.mpp.mpg.de/
[6] http://www.magic.iac.es/

Figure 2: The MAGIC Florian Goebel telescopes at the Roque de Los Muchachos Observatory, Spain. Image Credit: Chiara Righi.

4.2 Mirrors

Each telescope has an active mirroring surface of 236 m^2 and the squared mirror elements are of dimensions 49.5 × 49.5 cm for MAGIC-I; and 99 × 99 cm for the MAGIC-II dish. Each squared mirror element has an average reflectivity of approximately 80%. Mirror elements are made of glass and aluminium, supported by high quality materials such as quartz coating for protection from the outside effects. Furthermore, heating systems are implemented behind the squared mirrors in order to avoid icing and dew. Diameter of the parabolas is $\sim$ 17 m, focal length to diameter ration is f/D = 1.03. Each mirror panel is mounted on three points, of which one is a fixed point and two which are computer-controlled via Active Mirror Control system. Panels can be moved in every direction.

4.3 Structure

Construction made for mobility of the telescopes consists of six bogeys positioned on a circular rail. The rotation of the telescopes is defined by two axis: a horizontal one for adjusting the elevation, and a vertical one for adjusting the azimuth. For azimuthal movements they are equipped with two electric motors with power of 11 kW for each one. The telescopes are exceptionally agile - alternating from any point to the other takes no longer than 40 seconds.

5 JetSet program

For my study I have installed and used the program JetSeT [18, 19]. JetSeT was developed to model SEDs of AGNs and blazars. It is based on C and Python languages and it is publicly available. In JetSeT we can use several theoretical models to describe the broadband SED of sources, in my case I focused on the simplest one, a pure leptonic model named Synchrotron Self Compton [SSC, 20, 21, 22].

5.1 SSC model

Synchrotron self Compton (SSC) is a leptonic model combined of both synchrotron radiation and inverse Compton scattering.

Most of the non-thermal radio emission comes from Synchrotron emission of a population of electrons rotating in the magnetic field of the object. Force exerted on the electron:

$$\mathbf{F} = \frac{q(\mathbf{v} \times \mathbf{B})}{c}$$

It is the form of electromagnetic radiation which occurs when relativistic particles are accelerated in the presence of magnetic field perpendicular to particle's velocity. Polarization is notably linear for AGNs. Average power emitted by the electron:

$$\overline{P} = \frac{4}{3}\sigma_T c \gamma^2 \beta^2 u_B$$

Inverse Compton emission is based on high energy, relativistic electrons colliding with low energy photons (e.g. with radio frequencies) resulting in giving them higher energies. This produces high-energy radiation. Average power emitted by the electron:

$$\overline{P} = \frac{4}{3}\sigma_T c \gamma^2 \beta^2 u_{rad}$$

We notice that the power emitted from synchrotron process and the inverse Compton process are almost identical. The only difference here is we no longer observe energy density of the magnetic field u_B, but energy density of the radiation field u_{rad}. In a compact synchrotron source, the emitted photons can be inverse Compton scattered by the relativistic electrons that emit the synchrotron radiation. The synchrotron self-Compton process can continue within a source through additional scattering of photons until the limit is reached.

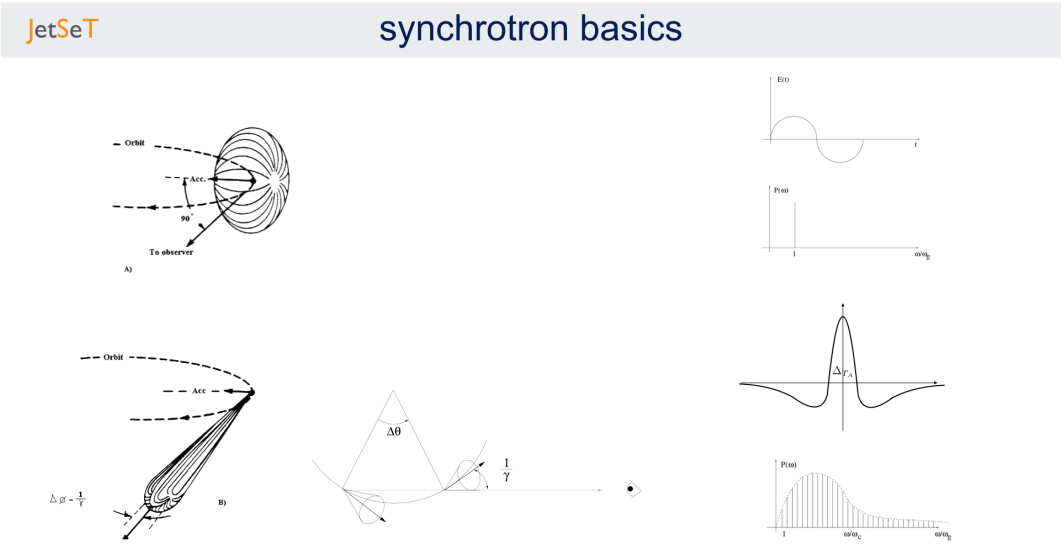

Figure 3: Synchrotron emission basics, illustration from `https://jetset.readthedocs.io/en/1.3.0/user_guide/documentation_notebooks/notebooks/phen_constr/SSC_th_bkg.html`

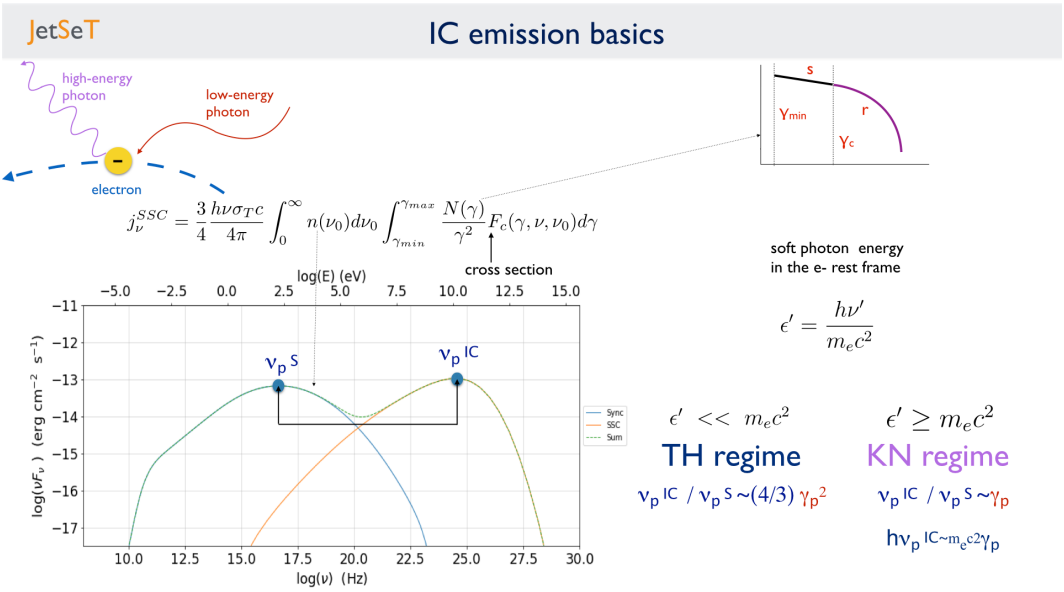

Figure 4: Inverse Compton emission basics illustration from `https://jetset.readthedocs.io/en/1.3.0/user_guide/documentation_notebooks/notebooks/phen_constr/SSC_th_bkg.html`

6 Results

In my trials, I used the parameters of [17] as a starting point. I set the jet Doppler factor δ to 25 and the magnetic field B in a range from 0.001 to 0.1 G. For both Phases, it is impossible to describe the high energy bump of the SED with the SSC model. The synchrotron peak can be nicely reproduced but the whole dataset is not reproducible by SSC.

6.1 Phase A

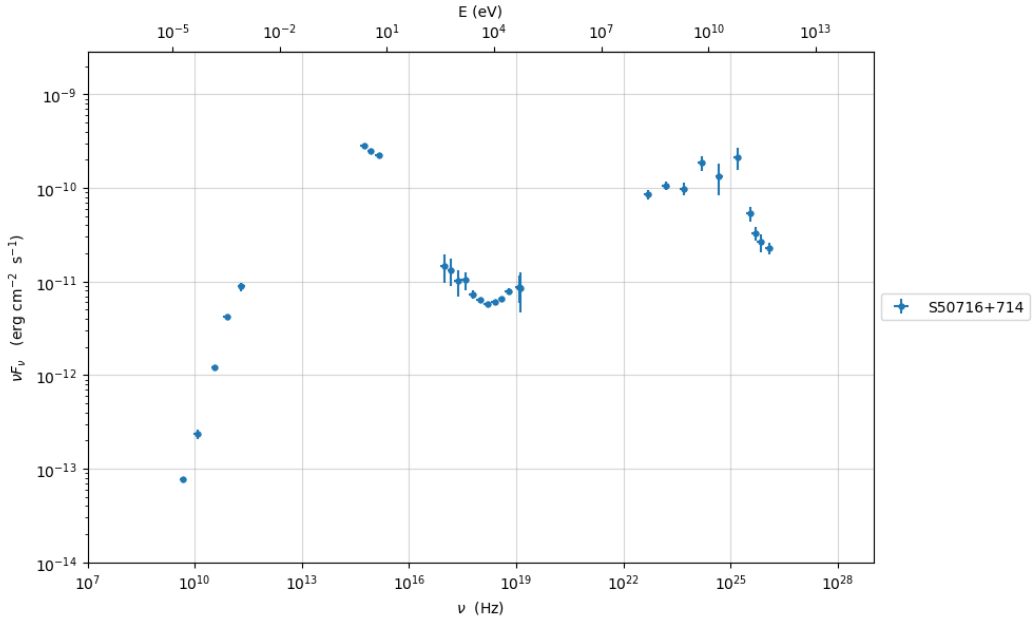

Figure 5: MWL data of S5 0716+714 during Phase A of the 2015 flaring activity.

In Fig. 5 the broadband SED of S5 0716+714 during Phase A, from MJD 57040 (18/01/2015) to MJD 57050 (27/01/2015) is shown. The datapoints were published in [17].

In Fig. 6, the indexes of the various energy bands for Phase A are calculated by JeTSeT. They will be used to start a preliminary polynomial fit to the SED.

With the polynomial fit, JeTSeT identifies the synchrotron and the IC peaks, which will be used in the next step of the program to produce the model. The polynomial fits are shown in Fig. 7.

The final model for Phase A is shown in Fig. 8.

The parameters of the model are listed in Fig. 9.

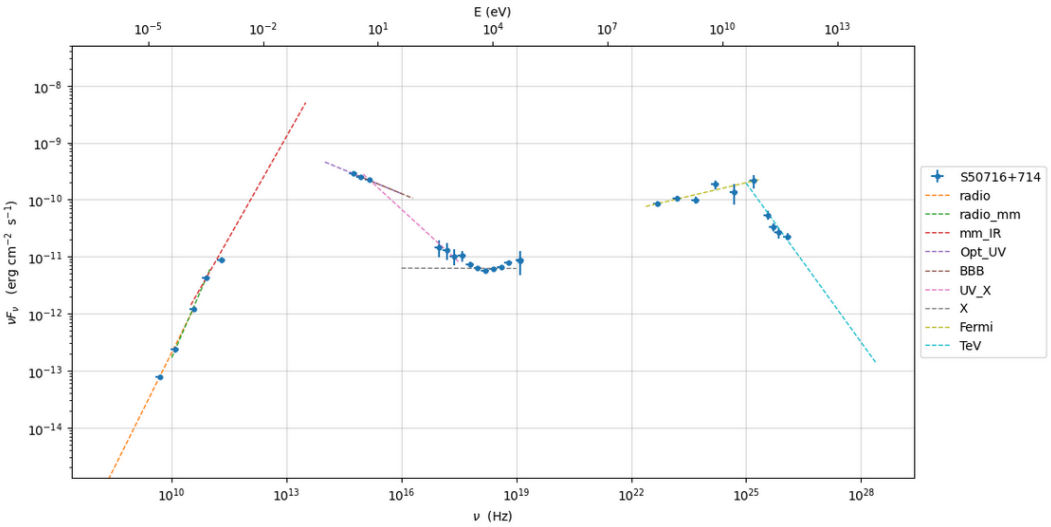

Figure 6: Indexes of the JeTSeT model fitting for Phase A.

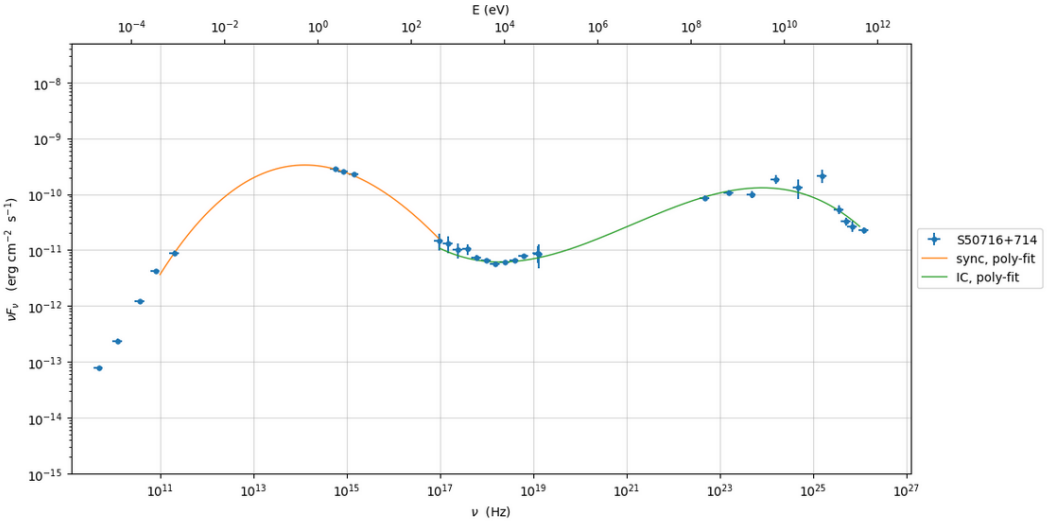

Figure 7: Polynomial fits to identify the peaks in the SEDs for Phase A.

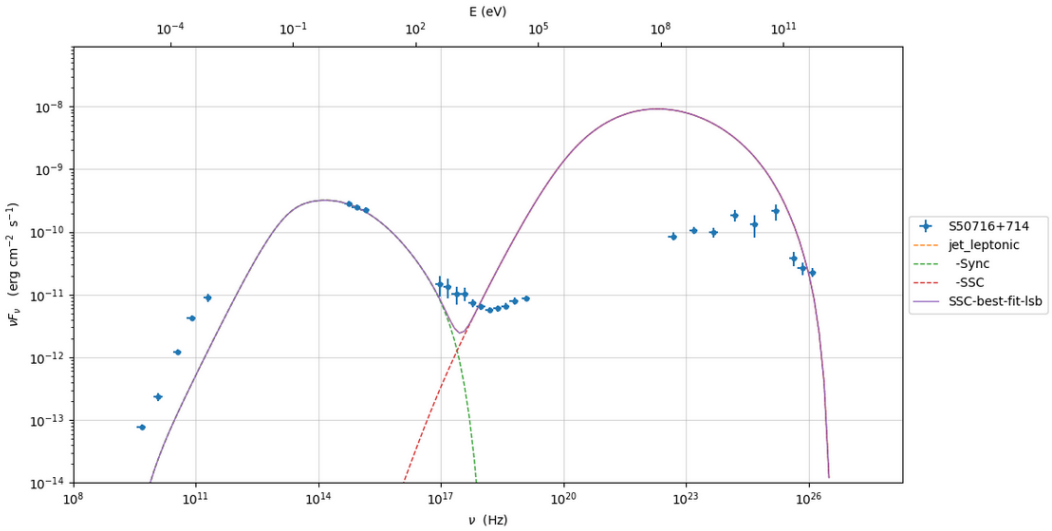

Figure 8: The SSC model superimposed to the dataset of Phase A.

name	par type	units	val	phys. bound. min	phys. bound. max	log	frozen
R	region_size	cm	4.943143e+16	1.000000e+03	1.000000e+30	False	False
R_H	region_position	cm	1.000000e+17	0.000000e+00	--	False	True
B	magnetic_field	gauss	5.050000e-02	0.000000e+00	--	False	False
NH_cold_to_rel_e	cold_p_to_rel_e_ratio		1.000000e+00	0.000000e+00	--	False	True
beam_obj	beaming		2.500000e+01	1.000000e-04	--	False	False
z_cosm	redshift		3.100000e-01	0.000000e+00	--	False	False
gmin	low-energy-cut-off	lorentz-factor*	1.674631e+03	1.000000e+00	1.000000e+09	False	False
gmax	high-energy-cut-off	lorentz-factor*	1.634241e+05	1.000000e+00	1.000000e+15	False	False
N	emitters_density	1 / cm3	5.339385e+01	0.000000e+00	--	False	False
gamma0_log_parab	turn-over-energy	lorentz-factor*	1.229181e+02	1.000000e+00	1.000000e+09	False	False
s	LE_spectral_slope		-1.235604e-01	-1.000000e+01	1.000000e+01	False	False
r	spectral_curvature		8.978803e-01	-1.500000e+01	1.500000e+01	False	False

Figure 9: Parameters of the SSC model for Phase A.

6.2 Phase B

In Fig. 10 the broadband SED of S5 0716 during Phase B, from MJD 57065 (12/02/2015) to MJD 57070 (17/02/2015) is shown. The datapoints were published in [17].

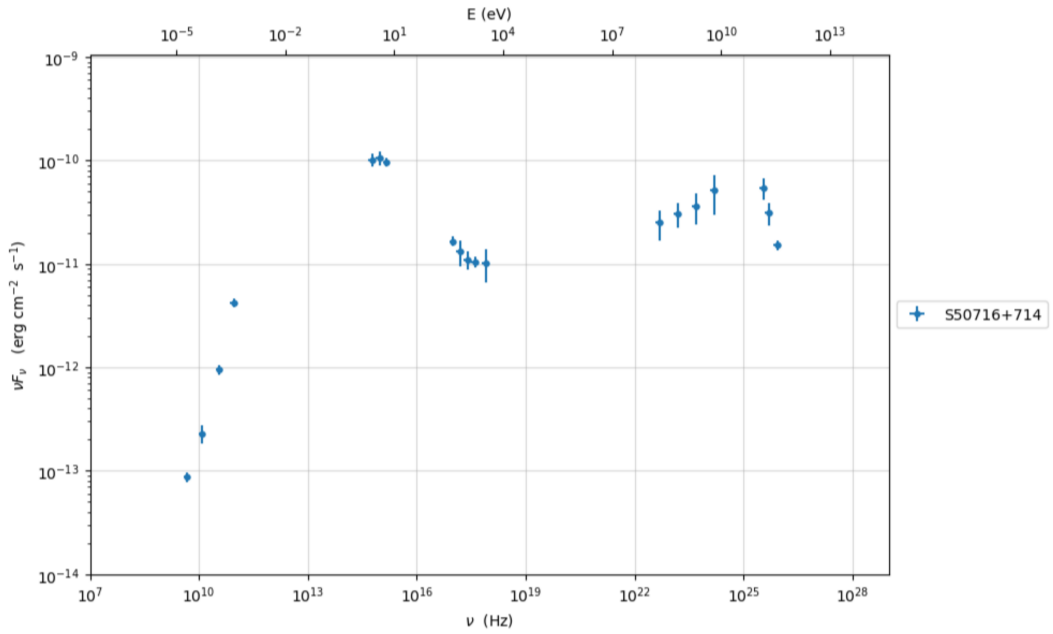

Figure 10: MWL data of S5 0716+714 during Phase B of the 2015 flaring activity.

In Fig. 11, the indexes of the various energy bands for Phase B are calculated by JeTSeT. They will be used to start a preliminary polynomial fit to the SED.

With the polynomial fit, JeTSeT identifies the synchrotron and the IC peaks, which will be used in the next step of the program to produce the model. The polynomial fits are shown in Fig. 12.

The final model for Phase B is shown in Fig. 13.

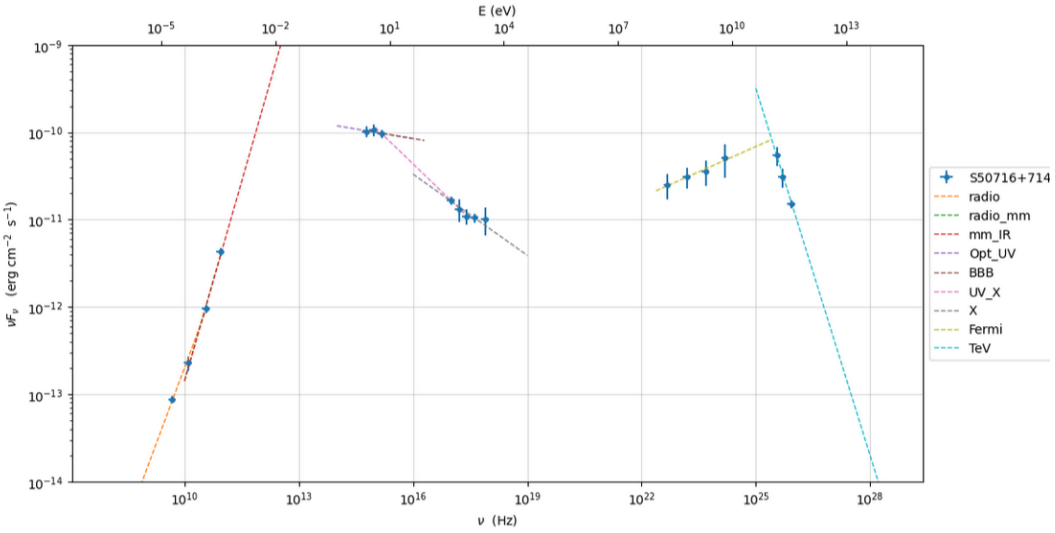

Figure 11: Indexes of the JeTSeT model fitting for Phase B.

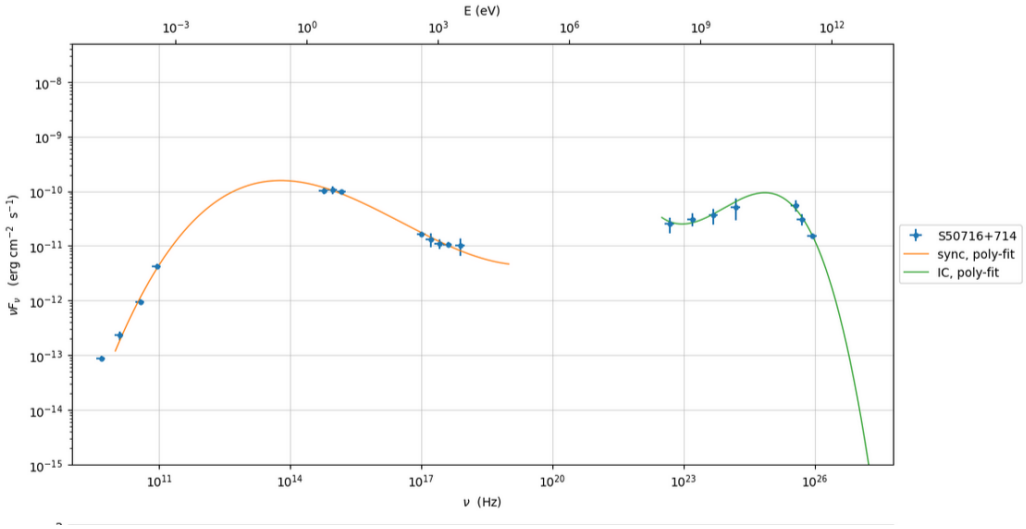

Figure 12: Polynomial fits to identify the peaks in the SEDs for Phase B.

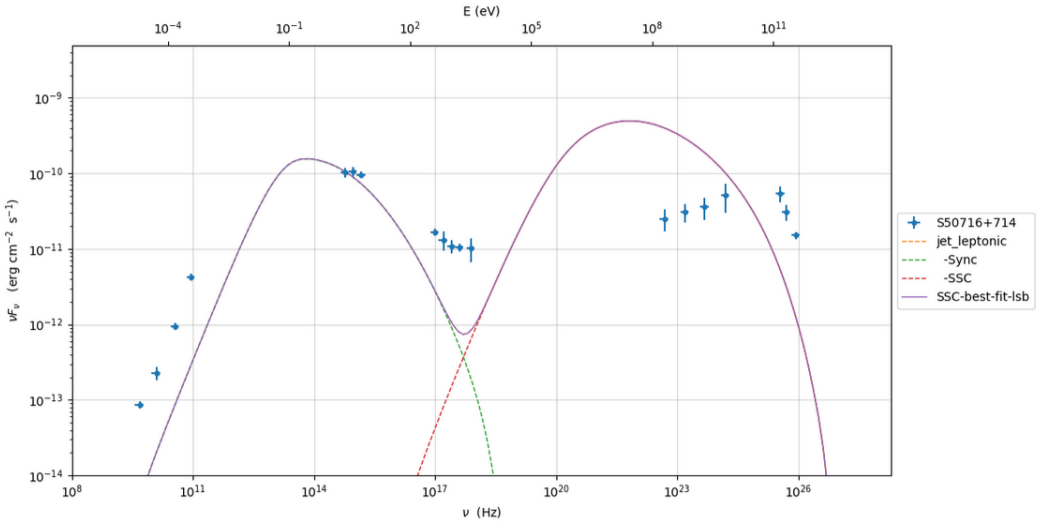

Figure 13: The SSC model superimposed to the dataset of Phase B.

name	par type	units	val	phys. bound. min	phys. bound. max	log	frozen
R	region_size	cm	9.886286e+16	1.000000e+03	1.000000e+30	False	False
R_H	region_position	cm	1.000000e+17	0.000000e+00	--	False	True
B	magnetic_field	gauss	5.050000e-02	0.000000e+00	--	False	False
NH_cold_to_rel_e	cold_p_to_rel_e_ratio		1.000000e+00	0.000000e+00	--	False	True
beam_obj	beaming		2.500000e+01	1.000000e-04	--	False	False
z_cosm	redshift		3.100000e-01	0.000000e+00	--	False	False
gmin	low-energy-cut-off	lorentz-factor*	1.674631e+03	1.000000e+00	1.000000e+09	False	False
gmax	high-energy-cut-off	lorentz-factor*	4.700048e+05	1.000000e+00	1.000000e+15	False	False
N	emitters_density	1 / cm3	4.175746e+00	0.000000e+00	--	False	False
gamma0_log_parab	turn-over-energy	lorentz-factor*	3.824906e+01	1.000000e+00	1.000000e+09	False	False
s	LE_spectral_slope		-4.682023e-02	-1.000000e+01	1.000000e+01	False	False
r	spectral_curvature		7.495900e-01	-1.500000e+01	1.500000e+01	False	False

Figure 14: Parameters of the SSC model for Phase B.

7 Conclusions

In this work, I tested the SSC model on the broadband SED of the blazar S5 0716+714, during a period of intense flaring activity in many energy bands in 2015. For my tests, I used the program JeTSeT and made two jupyter notebooks in python to model the SEDs of Phase A and B. The results show that this dataset can not be described by a one-zone SSC model. More complex models, probably including hadronic components, should be employed to reproduce the dataset and shed light on the emission mechanism of the source during this bright flare.

References

[1] Harris, G.L., Rejkuba, M. and Harris, W.E. The distance to ngc 5128 (centaurus a). *Publications of the Astronomical Society of Australia*, 27 (4):457–462, 2010.

[2] Wang, F. et al. A luminous quasar at redshift 7.642. *The Astrophysical Journal Letters*, 907(1):L1, 2021.

[3] Savolainen, T. et al. Relativistic beaming and gamma-ray brightness of blazars. *Astronomy & Astrophysics*, 512:A24, 2010.

[4] Thorne, J. *Lighting the Night: The Spectral Energy Distributions of Galaxies*. PhD thesis, The University of Western Australia, 2023. URL `https://research-repository.uwa.edu.au/en/publications/lighting-the-night-the-spectral-energy-distributions-of-galaxies`.

[5] Falomo, R. Host galaxy and close environment of bl lacertae objects. *Monthly Notices of the Royal Astronomical Society*, 283(1):241–250, 1996.

[6] Ghisellini, G. et al. The Fermi blazar sequence. *Monthly Notices of the Royal Astronomical Society*, 469(1):255–266, Jul 2017. doi: 10.1093/mnras/stx806.

[7] Wakely, S.P. and Horan, D. TeVCat: An online catalog for Very High Energy Gamma-Ray Astronomy. In *International Cosmic Ray Conference*, volume 3 of *International Cosmic Ray Conference*, pages 1341–1344, January 2008.

[8] Urry, C.M. and Padovani, P. Unified schemes for radio-loud active galactic nuclei. *Publications of the Astronomical Society of the Pacific*, 107 (715):803, 1995.

[9] Jiang, D. et al. Evn+merlin observations of bl lac object 1400+162. *New Astronomy Reviews*, 43(8):703–705, 1999. ISSN 1387-6473. doi: https://doi.org/10.1016/S1387-6473(99)00082-2. URL `https://www.sciencedirect.com/science/article/pii/S1387647399000822`.

[10] Giommi, P. et al. Synchrotron and inverse compton variability in the bl lacertae object s5 0716+ 714. *arXiv preprint astro-ph/9909241*, 1999.

[11] Ahnen, M.L. et al. Multi-wavelength characterization of the blazar s5 0716+714 during an unprecedented outburst phase. *Astronomy*

amp; Astrophysics, 619:A45, November 2018. ISSN 1432-0746. doi: 10.1051/0004-6361/201832677. URL `http://dx.doi.org/10.1051/0004-6361/201832677`.

[12] Nilsson, K. et al. Detection of the host galaxy of S5 0716+714. *Astronomy and Astrophysics*, 487(2):L29–L32, August 2008. doi: 10.1051/0004-6361:200810310.

[13] Rani, B. et al. Quasi-periodic Oscillations of ~15 Minutes in the Optical Light Curve of the BL Lac S5 0716+714. *The Astrophysical Journal Letters*, 719(2):L153–L157, August 2010. doi: 10.1088/2041-8205/719/2/L153.

[14] Rani, B. et al. Connection between inner jet kinematics and broadband flux variability in the bl lacertae object s5 0716+ 714. *Astronomy & Astrophysics*, 578:A123, 2015.

[15] Wagner, S. et al. Rapid variability in s5 0716+ 714 across the electromagnetic spectrum. *Astronomical Journal v. 111, p. 2187*, 111:2187, 1996.

[16] Bach, U. et al. Kinematic study of the blazar s5 0716+ 714. *Astronomy & Astrophysics*, 433(3):815–825, 2005.

[17] MAGIC Collaboration et al. Multi-wavelength characterization of the blazar S5 0716+714 during an unprecedented outburst phase. *Astronomy and Astrophysics*, 619:A45, November 2018. doi: 10.1051/0004-6361/201832677.

[18] Tramacere, A., Massaro, E. and Taylor, A.M. Stochastic Acceleration and the Evolution of Spectral Distributions in Synchro-Self-Compton Sources: A Self-consistent Modeling of Blazars' Flares. *The Astrophysical Journal*, 739(2):66, October 2011. doi: 10.1088/0004-637X/739/2/66.

[19] Tramacere, A. et al. Swift observations of the very intense flaring activity of Mrk 421 during 2006. I. Phenomenological picture of electron acceleration and predictions for MeV/GeV emission. *Astronomy and Astrophysics*, 501(3):879–898, July 2009. doi: 10.1051/0004-6361/200810865.

[20] Konigl, A. Relativistic jets as X-ray and gamma-ray sources. *The Astrophysical Journal*, 243:700–709, February 1981. doi: 10.1086/158638.

[21] Band, D.L. and Grindlay, J.E. The synchrotron-self-Compton process in spherical geometries. I - Theoretical framework. *The Astrophysical Journal*, 298:128–146, November 1985. doi: 10.1086/163593.

[22] Marscher, A.P. and Gear, W.K. Models for high-frequency radio outbursts in extragalactic sources, with application to the early 1983 millimeter-to-infrared flare of 3c 273. *The Astrophysical Journal*, 298: 114–127, 1985.